Communication

Broadband, Stable, and Noniterative Dielectric Constant Measurement of Low-Loss Dielectric Slabs Using a Frequency-Domain Free-Space Method

Ugur C. Hasar, Yunus Kaya, Gokhan Ozturk, Mehmet Ertugrul, and Celal Korasli

***Abstract*— A broadband, stable, and noniterative free-space method is proposed for dielectric constant ε_r' determination of low-loss dielectric slabs from reflection-only measurements through simple calibration standards (reflect and air). It is applicable for dispersive samples and does not require thickness information. Simulations of nondisperive and dispersive samples are performed to validate our method. Dielectric constant measurements of polyethylene and polyoxymethylene samples (9–11 GHz) are carried out to examine the accuracy of our method.**

***Index Terms*— Dispersive, free-space, frequency-domain, nondispersive, noniterative, reflection-only, simple calibration.**

I. Introduction

Characterization of materials can be indirectly implemented by measuring permittivity $\varepsilon_r = \varepsilon_r' - i\varepsilon_r''$, since such a response is an intrinsic property of and thus unique to each material. Sufficient information about such a response of a material can be gained by wideband measurements at microwave frequencies [1], [2], [3], [4], [5], [6], [7], [8], [9], [10], [11] using the coaxial-line (or waveguide) method, the planar transmission-line method, and the free-space method. Among these methods, the free-space methods are nondestructive, contactless, and applicable for measurements at high temperatures.

There are some issues related to free-space techniques. First, these techniques require exact knowledge of the sample thickness prior to material characterization [12], [13], [14], [15], [16], [17]. The free-space techniques in the studies [18], [19], [20] can be used to determine electromagnetic properties of materials without using their thickness information. However, the method in [18], which is based on oscillatory behavior of wideband measured reflection/transmission measurements [9], [21], [22], is restricted to nondispersive or weakly dispersive materials and thus is not applicable for dispersive samples. Besides, the method in [19], as will be shown in Section III, can introduce undesired ripples in the extracted dielectric constant (ε_r') of thicker low-loss samples or samples with higher ε_r' over broadband measurements. On the other hand, the method in [20] is not applicable for narrowband frequency measurements. Second, free-space techniques relying on numerical techniques could result in erroneous results if an initial guess for material properties is not properly given near the global minimum [23]. The noniterative techniques in the studies [15], [17] could be applied for noniterative ε_r determination. Nonetheless, they necessitate that the measurement and calibration planes overlap each other and consequently are seriously affected by any shift between these planes (dependence on reference planes) [9]. Third, free-space techniques generally use both reflection and transmission scattering (S-)parameter measurements to determine electromagnetic properties of the sample. Nevertheless, transmission measurements are not adequate for electromagnetic characterization of samples whose backs are not accessible [16], [17]. Besides, any misalignment of transmitting and receiving antennas can reduce measurement accuracy for transmission free-space S-parameter measurements. Both these situations direct one to perform electromagnetic characterization of samples using reflection-only S-parameter measurements [16], [17], [19]. Finally, free-space techniques generally employ calibration techniques such as the thru-reflect-line [24] or thru-reflect-match [25] to calibrate the measurement system before carrying out free-space measurements. Improper application of such calibration techniques can rather limit the accuracy of free-space measurements [11], [12], [13], [15], [18], similar to waveguide measurements [9].

In our recent study, we have proposed a microwave method for noniterative ε_r measurement of dielectric samples using reference-plane-invariant reflection-only time-domain S-parameters without knowing the sample thickness [26]. However, this method requires that ε_r of the sample be not changing or slightly changing with frequency and thus is applicable for nondispersive or weakly dispersive materials. In this study, we propose another free-space measurement technique (simple and accurate) for noniterative accurate ε_r' determination of dispersive/nondispersive low-loss dielectric samples at one frequency (frequency-to-frequency determination) without resorting to their thickness information using uncalibrated reference-plane-invariant reflection-only frequency-domain S-parameter measurements.

II. Proposed Methodology

Fig. 1 illustrates measurement configurations for ε_r' measurement of a dielectric sample by our method. The configuration in Fig. 1(a) shows the horn-lens antenna, fed from a rectangular waveguide operated at its TE_{10} (dominant mode), radiating into the air without any border. For this configuration, measured reflection coefficient Γ_{air} can be written as [19], [27]

$$\Gamma_{\text{air}} = \Gamma_0 \tag{1}$$

which considers (multiple) reflections within lens-horn antenna and from the connection of waveguide and horn antenna.

Besides, the configuration in Fig. 1(b) illustrates the same horn-lens antenna terminated in a large highly reflective metal plate located

Manuscript received 27 January 2022; revised 3 September 2022; accepted 16 September 2022. Date of publication 3 October 2022; date of current version 22 December 2022. This work was supported in part by the Scientific and Technological Research Council of Türkiye (TUBITAK) under Project 218M341. *(Corresponding author: Ugur C. Hasar.)*

Ugur C. Hasar is with the Department of Electrical and Electronics Engineering, Gaziantep University, 27310 Gaziantep, Türkiye (e-mail: uchasar@gantep.edu.tr).

Yunus Kaya is with the Department of Electricity and Energy, Bayburt University, 69000 Bayburt, Türkiye.

Gokhan Ozturk is with the Department of Electrical and Electronics Engineering, Ataturk University, 25240 Erzurum, Türkiye.

Mehmet Ertugrul is with the Department of Electrical and Electronics Engineering, Ataturk University, 25240 Erzurum, Türkiye, also with the Department of Electrical and Electronics Engineering, Universiti Putra Malaysia (UPM), Serdang, Selangor 43400, Malaysia, and also with the Department of Electric and Electronics Engineering, Kyrgyz Turkish Manas University, Bishkek 720044, Kyrgyzstan.

Celal Korasli is with the Department of Electrical and Electronics Engineering, Hasan Kalyoncu University, 27410 Gaziantep, Türkiye.

Color versions of one or more figures in this communication are available at https://doi.org/10.1109/TAP.2022.3209712.

Digital Object Identifier 10.1109/TAP.2022.3209712

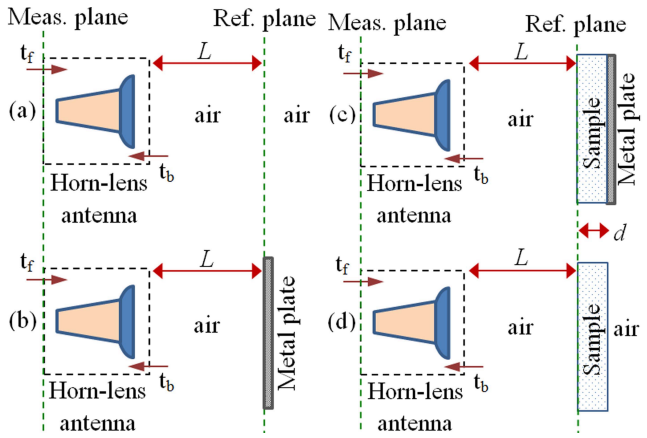

Fig. 1. Measurement configurations in the application of our proposed method. (a) Horn-lens antenna radiating into free space. (b) Same antenna terminated in a large highly reflective metal plate in the far zone (L distance from the reference plane). (c) Same antenna radiating into metal-backed sample with length d. (d) Same antenna radiating into the air-backed sample.

at the distance L (reference plane) in the far-zone of the horn-lens antenna. Assuming that there is perfect reflection from the metal plate, the reflection coefficient Γ_{metal} for this configuration can be expressed as [19], [27]

$$\Gamma_{\text{metal}} \cong \Gamma_0 - t_f t_b T_0^2, \quad T_0 = e^{-ik_0 L} \tag{2}$$

where t_f and t_b are the forward and backward transmission terms for wave transmissions into horn-lens antenna, as shown in Fig. 1, T_0 is the propagation factor for one-way travel in the air between the horn-lens antenna and metal plate, and k_0 is the free-space wavenumber. It is assumed that multiple reflections between the horn-lens antenna and the metal plate are assumed to be small or can be neglected. Using the measurements in Fig. 1(a) and (b), it is possible to determine

$$t_f t_b T_0^2 \cong \Gamma_{\text{air}} - \Gamma_{\text{metal}}. \tag{3}$$

On the other hand, Fig. 1(c) and (d) demonstrates the configurations for the metal- and air-backed sample with length d, where the sample front face coincides with the reference plane. For these configurations, the reflection coefficients $\Gamma_{\text{metal-back}}$ and $\Gamma_{\text{air-back}}$ can be written as

$$\Gamma_{\text{metal-back}} \cong \Gamma_0 + t_f t_b T_0^2 \left(r_{12} - T^2\right) / \left(1 - r_{12} T^2\right) \tag{4}$$

$$\Gamma_{\text{air-back}} \cong \Gamma_0 + t_f t_b T_0^2 r_{12}(1 - T^2) / \left(1 - r_{12}^2 T^2\right) \tag{5}$$

$$r_{12} = \left(1 - \sqrt{\varepsilon_r}\right) / \left(1 + \sqrt{\varepsilon_r}\right), \quad T = e^{-ik_0\sqrt{\varepsilon_r} d}. \tag{6}$$

Here, r_{12} is the reflection coefficient from air to the sample, and T is the propagation factor within the sample. It is noted that as different from the methods in [27] and [28], our method considers multiple reflections within the sample.

Incorporating (3) into (4) and (5), one can evaluate

$$\frac{\Gamma_{\text{air-back}} - \Gamma_{\text{air}}}{\Gamma_{\text{air}} - \Gamma_{\text{metal}}} \cong \Lambda_1 = \frac{r_{12}(1 - T^2)}{1 - r_{12}^2 T^2} \tag{7}$$

$$\frac{\Gamma_{\text{metal-back}} - \Gamma_{\text{air}}}{\Gamma_{\text{air}} - \Gamma_{\text{metal}}} \cong \Lambda_2 = \frac{r_{12} - T^2}{1 - r_{12} T^2} \tag{8}$$

where Λ_1 and Λ_2 are the terms related to measured quantities. Then, after eliminating the common term T^2 from (7) and (8), it is possible to calculate r_{12} as

$$r_{12} = -\chi \mp \sqrt{\chi^2 - 1}, \quad \chi = \left[\frac{(\Lambda_1 - 1) - (\Lambda_1 + 1)\Lambda_2}{2\Lambda_1}\right]. \tag{9}$$

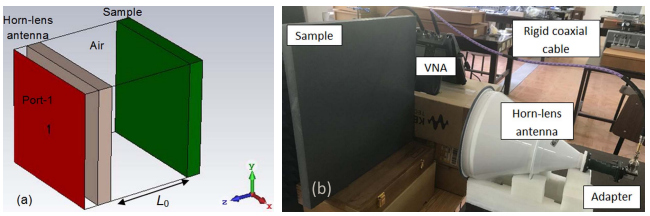

Fig. 2. (a) Computational environment for the configuration in Fig. 1(c) and (b) a photograph of the measurement setup for validation of our method.

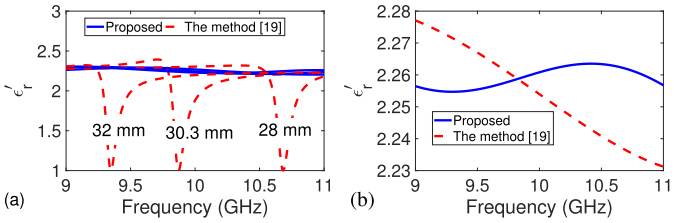

Fig. 3. Extracted ε_r' of the PP sample with (a) $d = 28$, 30.3, and 32 mm and (b) $d = 5.0$ mm by the proposed method and the method in [19].

The correct sign for r_{12} can be evaluated by using the passivity principle, that is, $|r_{12}| \leq 1$, where $|\star|$ denotes the magnitude of "$\star$." Finally, ε_r' can be retrieved from

$$\varepsilon_r' = \Re e\left\{ (1 - r_{12})^2 / (1 + r_{12})^2 \right\}. \tag{10}$$

It is seen from (1)–(10) that our method is noniterative does not require information of d, extracts ε_r' at any frequency (applicable for dispersive materials as validated by simulations in Section III) within a broadband and uses only reflection measurements from simple calibration standards (see Fig. 1).

III. Simulation and Validation

For validation of our method, we performed simulations using a commercial full-wave electromagnetic simulation program [the computer simulation technology (CST)—Microwave Studio (MWS)]. In the validation, a planar slab (50 × 50 mm cross section) with $\varepsilon_{ra} = 1.2 - i0.0002$ (to reduce multiple reflections between antennas and the metal plate) and a length of 1.0 mm was considered to simulate, for simplicity, the horn-lens antenna region in Fig. 1. The discussion of the elimination of these reflections is given in Section IV. Besides, planar low-loss samples (40 × 40 mm cross section) with $\varepsilon_r = 2.26 - i0.00008$ [the polyethylene (PP)] [29]) and $d = 30.3$ mm (or $d = 32$, 28, or 5.0 mm), with $\varepsilon_r = 20.0 - i0.00008$ and $d = 30.0$ mm, and with ε_r synthesized by the Debye model and $d = 30.0$ mm were considered as the samples. The PP sample was simulated to compare its extracted ε_r' from measurements for $L = 30.0$ cm (see Section IV). To simulate plane wave propagation, $E_t = 0$ and $H_t = 0$ boundary conditions were set over transverse planes. A waveguide port was applied to excite the computational environment and to obtain S-parameters. For the configurations in Fig. 1(b) and (c), $E_t = 0$ boundary condition was also set to simulate the metal plate. The frequency range was arranged by the operating frequency range of the horn-lens antenna as 9–11 GHz. Besides, the adaptive mesh refinement option was activated to get optimum meshing. Fig. 2(a) illustrates the computational environment for the configuration in Fig. 1(c).

Our method was then applied to determine ε_r' of the examined samples using their simulated S-parameters of the configurations in Fig. 1. In addition, we also applied the method in [19] to retrieve ε_r' of these samples. Fig. 3(a) demonstrates the extracted ε_r' of the

TABLE I

EXTRACTED ε_r' OF THE PP SAMPLE ($d = 30.3$ mm) FROM SIMULATION

Frequency (GHz)	Proposed method ε_r'	Proposed method $\Delta\varepsilon_r'(\%)$	The method in [19] ε_r'	The method in [19] $\Delta\varepsilon_r'(\%)$
9.00	2.298	1.694	2.292	1.432
9.25	2.301	1.790	2.310	2.185
9.50	2.289	1.272	2.344	3.721
9.75	2.267	0.331	2.375	5.085
10.00	2.243	0.748	1.891	16.570
10.25	2.222	1.646	2.136	5.446
10.50	2.212	2.108	2.190	3.034
10.75	2.217	1.902	2.214	2.052
11.00	2.236	1.072	2.225	1.536

TABLE II

EXTRACTED ε_r' OF THE PP SAMPLE ($d = 5.0$ mm) FROM SIMULATION

Frequency (GHz)	Proposed method ε_r'	Proposed method $\Delta\varepsilon_r'(\%)$	The method in [19] ε_r'	The method in [19] $\Delta\varepsilon_r'(\%)$
9.00	2.256	0.156	2.277	0.756
9.25	2.255	0.232	2.273	0.555
9.50	2.255	0.202	2.267	0.309
9.75	2.258	0.095	2.261	0.031
10.00	2.261	0.040	2.254	0.270
10.25	2.263	0.134	2.247	0.562
10.50	2.263	0.150	2.241	0.847
10.75	2.261	0.057	2.235	1.093
11.00	2.257	0.143	2.231	1.274

PP sample with $d = 28$, 30.3, and 32 mm by our method and the method in [19]. It is seen from Fig. 3(a) that extracted ε_r' by the method in [19] mainly diverges from the preassigned one especially within the frequency bands over which the thickness resonance effect arising when $\varepsilon_r'' \to 0$ dominates [30], [31], that is, $d = n\lambda/2$, where n denotes an integer. On the other hand, extracted ε_r' by our method is in good agreement with the preassigned one for each d, except for a small deviation which is mainly due to the simplified model for the horn-lens antenna represented by t_f and t_b terms only. This indicates that our method is not affected by the thickness resonance effect thanks to simultaneous usage of air-backed and metal-backed measurements [30], [31]. For a quantitative analysis, Table I shows extracted ε_r' of the PP sample with $d = 30.3$ mm by our method and the method in [19] together with percentage errors $\Delta\varepsilon_r'$ at some discrete frequencies ($\Delta f = 250$ MHz). It is seen from Table I that while $\Delta\varepsilon_r' \leq 2.108\%$ for our method, $\Delta\varepsilon_r'$ for the method in [19] can reach up to 16.57%.

To evaluate the performance of our method and the method [19] for frequencies away from the thickness-resonance region, we extracted ε_r' of the PP sample with $d = 5.0$ mm by these methods, as shown in Fig. 3(b). It is seen from Fig. 3(b) that our method and the method [19] have similar accuracy. For a quantitative analysis, the extracted ε_r' and $\Delta\varepsilon_r'$ values for our method and the method in [19] are presented in Table II. It can be noticed from Table II that extracted ε_r' values by our method and the method in [19] are individually very close to the preassigned one ($\Delta\varepsilon_r' \leq 1.28\%$ for both methods). A similar conclusion was also noted for the polyoxymethylene (POM) sample with $\varepsilon_r = 2.73 - i0.00513$ [29], whose results are not presented for conciseness. On the other hand, Fig. 4(a) and Table III exhibit extracted ε_r' of the sample with $\varepsilon_r = 20.0 - i0.00008$ and $d = 30.0$ mm by our method and the method in [19], together with $\Delta\varepsilon_r'$ values, to observe the effect of ε_{rs} on extraction procedures. It is seen from Fig. 4(a) and Table III that the accuracy of our method does not much change ($\Delta\varepsilon_r' \leq 4.195$), whereas that of the method in [19] significantly alters ($\Delta\varepsilon_r'$ can exceed 70% around 10.0 GHz due to thickness resonance effect) with an increase of ε_r'.

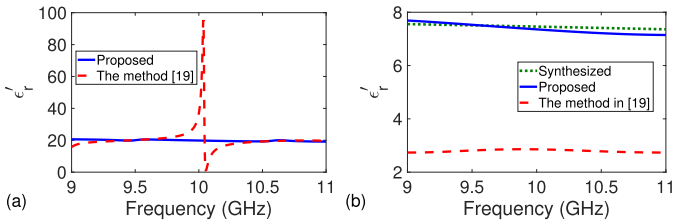

Fig. 4. Extracted ε_r' of (a) sample with $\varepsilon_r = 20.0 - i0.00008$ and $d = 30.0$ mm and (b) synthesized sample described via the Debye model by the proposed method and the method in [19].

TABLE III

EXTRACTED ε_r' OF THE SAMPLE WITH $\varepsilon_r = 20.0 - i0.00008$ AND $d = 5.0$ mm FROM SIMULATION

Frequency (GHz)	Proposed method ε_r'	Proposed method $\Delta\varepsilon_r'(\%)$	The method in [19] ε_r'	The method in [19] $\Delta\varepsilon_r'(\%)$
9.00	20.60	3.007	15.71	21.47
9.25	20.31	1.537	19.21	3.975
9.50	20.05	0.176	20.12	0.723
9.75	20.24	1.188	21.55	7.854
10.00	19.82	0.841	36.95	> 60
10.25	19.48	2.550	17.49	13.11
10.50	19.33	3.370	19.24	3.835
10.75	19.53	2.302	19.82	0.845
11.00	19.16	4.195	19.52	2.407

TABLE IV

EXTRACTED ε_r' OF THE SYNTHESIZED SAMPLE FROM SIMULATION

Frequency (GHz)	Proposed method ε_r'	Proposed method $\Delta\varepsilon_r'(\%)$	The method in [19] ε_r'	The method in [19] $\Delta\varepsilon_r'(\%)$
9.00	7.690	3.746	2.738	65.02
9.25	7.614	3.036	2.759	64.75
9.50	7.529	2.116	2.813	64.06
9.75	7.442	1.121	2.854	63.54
10.00	7.353	0.060	2.856	63.50
10.25	7.281	0.902	2.826	63.90
10.50	7.216	1.800	2.781	64.46
10.75	7.169	2.497	2.747	64.90
11.00	7.146	2.917	2.735	65.05

Finally, we also tested the applicability of our method for ε_r' determination of dispersive samples. To this end, we synthesized a sample using the Debye model [32] given by

$$\varepsilon_r = \varepsilon_\infty + (\varepsilon_s - \varepsilon_\infty) / (1 + i\ 2\pi f \tau) \tag{11}$$

where ε_s and ε_∞ are the relative permittivities at zero and infinite frequencies, and τ is the relaxation time. The sample was assumed to have $\varepsilon_s = 8.0$, $\varepsilon_\infty = 2.0$ ($\varepsilon_s > \varepsilon_\infty$), and $\tau = 5$ ps. Fig. 4(b) shows the synthesized and extracted ε_r' of the synthesized sample $d = 30.0$ mm by the proposed method and the method in [19]. It is seen from Fig. 4(b) that extracted ε_r' by our method produces results similar to that synthesized ε_r' by the Debye model, whereas the synthesized and extracted ε_r' by the method in [19] greatly differ from each other. It is seen from Table IV, which presents $\Delta\varepsilon_r'$ values for this sample, that $\Delta\varepsilon_r'$ for our method is less than 3.75%, that for the method in [19] is greater than 60%. Such a difference is mainly due to nonnegligible effect of ε_r'' on the extracted ε_r' by the method in [19].

IV. MEASUREMENTS AND DISCUSSION

Fig. 2(b) illustrates a photograph of the measurement setup used for validation of the proposed method. It consists of a vector network analyzer (VNA) with the model of N9918A from Keysight Technologies (30 kHz–26.5 GHz), a rigid coaxial line phase stable cable

TABLE V
EXTRACTED ε_r' OF THE PP SAMPLE FROM MEASUREMENT

Frequency (GHz)	Proposed method ε_r'	Proposed method $\Delta\varepsilon_r'(\%)$	The method in [9] ε_r'	The method in [9] $\Delta\varepsilon_r'(\%)$
9.00	2.13 ∓ 0.07	5.75	2.20 ∓ 0.06	2.65
9.25	2.17 ∓ 0.06	3.98	2.22 ∓ 0.06	1.77
9.50	2.21 ∓ 0.05	2.21	2.25 ∓ 0.05	0.44
9.75	2.19 ∓ 0.06	3.10	2.28 ∓ 0.04	0.88
10.00	2.18 ∓ 0.04	3.54	2.30 ∓ 0.06	1.77
10.25	2.14 ∓ 0.05	5.31	2.31 ∓ 0.05	2.21
10.50	2.32 ∓ 0.04	2.65	2.33 ∓ 0.04	3.10
10.75	2.15 ∓ 0.06	4.87	2.31 ∓ 0.04	2.21
11.00	2.31 ∓ 0.05	2.21	2.29 ∓ 0.04	1.33

TABLE VI
EXTRACTED ε_r' OF THE POM SAMPLE FROM MEASUREMENT

Frequency (GHz)	Proposed method ε_r'	Proposed method $\Delta\varepsilon_r'(\%)$	The method in [19] ε_r'	The method in [19] $\Delta\varepsilon_r'(\%)$
9.00	2.75 ∓ 0.06	0.73	2.84 ∓ 0.05	4.03
9.25	2.76 ∓ 0.05	1.10	2.80 ∓ 0.06	2.56
9.50	2.74 ∓ 0.05	0.37	2.75 ∓ 0.06	0.73
9.75	2.76 ∓ 0.04	1.10	2.77 ∓ 0.06	1.47
10.00	2.66 ∓ 0.06	2.56	2.65 ∓ 0.05	2.93
10.25	2.62 ∓ 0.05	4.03	2.67 ∓ 0.07	2.20
10.50	2.60 ∓ 0.07	4.76	2.84 ∓ 0.06	4.03
10.75	2.63 ∓ 0.05	3.66	2.86 ∓ 0.05	4.76
11.00	2.78 ∓ 0.04	1.83	2.87 ∓ 0.04	5.13

with a length of 100 cm, a coaxial-to-waveguide adapter operating at X-band (8.2–12.4 GHz), and a horn-lens antenna from Flann Microwave Instruments (Series 820) with 25 dB gain and maximum 1.5 VSWR over 9–11 GHz frequency range (for this reason, measurements were restricted to 9–11 GHz). The PP sample with $d = 30.3 \mp 0.3$ mm and the POM sample with $d = 30.0 \mp 0.3$ mm in a slab form (with 50×50 cm transverse area to reduce diffraction effects) were positioned away from the horn-lens antenna by $L = 30$ cm based on its focal distance to realize the plane wave assumption. Besides, the surfaces of the samples and the lens, positioned on a holder to remove floor scattering, were arranged parallel (normal incidence) to minimize any angle misalignment. Time-domain gating was applied for our method over the main reflection response of Γ_{metal} in Fig. 1(b) to reduce multiple reflections between the horn-lens antenna and the reference plane. Measurements were performed for 1001 frequency points and repeated three times.

Tables V and VI illustrate the extracted ε_r' over 9–11 GHz of the PP and POM samples by our method and the method in [19] [with time-domain gating over the main reflection response of Γ_{metal} in Fig. 1(b)] and the method in [9] using the average of five independent reflection-only measurements. It is seen from Tables V an VI that extracted ε_r' values by our method and the methods in [9] and [19] are in good agreement with the reference data [29]. It is noted from Table V that although the accuracy of our method ($\Delta\varepsilon_r' \leq 5.75\%$) is lower than that of the method ($\Delta\varepsilon_r' \leq 3.10\%$) in [9], our method is based on frequency-to-frequency determination and is a reference-plane-invariant method using uncalibrated measurements. Besides, it can be seen from Table VI that while the maximum value of $\Delta\varepsilon_r'$ is 4.76% for our method, the maximum value of $\Delta\varepsilon_r'$ is 5.13% for the method in [19], meaning that our method has better accuracy than the method in [19] because it does not consider $\varepsilon_r \to 0$ in the extraction. Finally, it should be stated that our method and the method in [9], as a drawback, require that the metal be backed right at the rear face of the sample in Fig. 1(c) without any gap.

V. CONCLUSION

An attractive broadband, stable, and noniterative free-space method is proposed for dielectric constant measurement of planar dielectric samples. It has the capability of extracting ε_r' of dispersive and nondispersive samples using reflection-only measurements through simple calibration standards (reflect and air) without resorting to any sample thickness information. CST MWS simulations were performed to assess the suitability of our method for nondispersive thicker low-loss samples and thinner/thicker dispersive samples. Measurements of ε_r' over 9–11 GHz of PP and POM samples were used to validate our method and examine its accuracy.

REFERENCES

[1] S. Trabelsi and S. O. Nelson, "Microwave sensing of quality attributes of agricultural and food products," *IEEE Instrum. Meas. Mag.*, vol. 19, no. 1, pp. 36–41, Feb. 2016.

[2] M. Ozturk, M. Karaaslan, O. Akgol, and U. K. Sevim, "Mechanical and electromagnetic performance of cement based composites containing different replacement levels of ground granulated blast furnace slag, fly ash, silica fume and rice husk ash," *Cement Concrete Res.*, vol. 136, Oct. 2020, Art. no. 106177.

[3] T. Mosavirik, M. Soleimani, V. Nayyeri, S. H. Mirjahanmardi, and O. M. Ramahi, "Permittivity characterization of dispersive materials using power measurements," *IEEE Trans. Instrum. Meas.*, vol. 70, pp. 1–8, 2021.

[4] H. Hasar et al., "Prediction of water-adulteration within honey by air-line de-embedding waveguide measurements," *Measurement*, vol. 179, Jul. 2021, Art. no. 109469.

[5] L. F. Chen, C. K. Ong, C. P. Neo, V. V. Varadan, and V. K. Varadan, *Microwave Electronics: Measurement and Materials Characterization*. West Sussex, U.K.: Wiley, 2004.

[6] A. M. Nicolson and G. F. Ross, "Measurement of the intrinsic properties of materials by time-domain techniques," *IEEE Trans. Instrum. Meas.*, vol. IM-19, no. 4, pp. 377–382, Nov. 1970.

[7] W. B. Weir, "Automatic measurement of complex dielectric constant and permeability at microwave frequencies," *Proc. IEEE*, vol. 62, no. 1, pp. 33–36, Jan. 1974.

[8] J. Baker-Jarvis, E. J. Vanzura, and W. A. Kissick, "Improved technique for determining complex permittivity with the transmission/reflection method," *IEEE Trans. Microw. Theory Techn.*, vol. 38, no. 8, pp. 1096–1103, Aug. 1990.

[9] C. Yang, H. Huang, and M. Peng, "Non-iterative method for extracting complex permittivity and thickness of materials from reflection-only measurements," *IEEE Trans. Instrum. Meas.*, vol. 71, pp. 1–8, 2022.

[10] M. A. H. Ansari, A. K. Jha, and M. J. Akhtar, "Design and application of the CSRR-based planar sensor for noninvasive measurement of complex permittivity," *IEEE Sensors J.*, vol. 15, no. 12, pp. 7181–7189, Dec. 2015.

[11] V. V. Varadan, R. D. Hollinger, D. K. Ghodgaonkar, and V. K. Varadan, "Free-space, broadband measurements of high-temperature, complex dielectric properties at microwave frequencies," *IEEE Trans. Instrum. Meas.*, vol. 40, no. 5, pp. 842–846, Oct. 1991.

[12] D. K. Ghodgaonkar, V. V. Varadan, and V. K. Varadan, "A free-space method for measurement of dielectric constants and loss tangents at microwave frequencies," *IEEE Trans. Instrum. Meas.*, vol. 38, no. 3, pp. 789–793, Jun. 1989.

[13] D. K. Ghodgaonkar, V. V. Varadan, and V. K. Varadan, "Free-space measurement of complex permittivity and complex permeability of magnetic materials at microwave frequencies," *IEEE Trans. Instrum. Meas.*, vol. 39, no. 2, pp. 387–394, Apr. 1990.

[14] A. Rashidian, L. Shafai, D. Klymyshyn, and C. Shafai, "A fast and efficient free-space dielectric measurement technique at mm-wave frequencies," *IEEE Antennas Wireless Propag. Lett.*, vol. 16, pp. 2630–2633, 2017.

[15] C. Yang, K. Ma, and J.-G. Ma, "A noniterative and efficient technique to extract complex permittivity of low-loss dielectric materials at terahertz frequencies," *IEEE Antennas Wireless Propag. Lett.*, vol. 18, no. 10, pp. 1971–1975, Oct. 2019.

[16] U. C. Hasar, G. Ozturk, M. Bute, and M. Ertugrul, "Method for electromagnetic property extraction of sublayers in metal-backed inhomogeneous metamaterials," *IEEE Access*, vol. 8, pp. 51718–151705, 2020.

[17] U. C. Hasar et al., "Feasible extraction method for electromagnetic properties of multilayer metamaterials with short-circuit termination," *IEEE Trans. Antennas Propag.*, early access, Aug. 8, 2022, doi: 10.1109/TAP.2022.3195500.
[18] S. Kim, D. Novotny, J. Gordon, and J. Guerrieri, "A free-space measurement method for the low-loss dielectric characterization without prior need for sample thickness data," *IEEE Trans. Antennas Propag.*, vol. 64, no. 9, pp. 3869–3879, Sep. 2016.
[19] L. Li, H. Hu, P. Tang, R. Li, B. Chen, and Z. He, "Compact dielectric constant characterization of low-loss thin dielectric slabs with microwave reflection measurement," *IEEE Antennas Wireless Propag. Lett.*, vol. 17, no. 4, pp. 575–578, Apr. 2018.
[20] Y. Yashchyshyn and K. Godziszewski, "A new method for dielectric characterization in sub-THz frequency range," *IEEE Trans. THz Sci. Technol.*, vol. 8, no. 1, pp. 19–26, Jan. 2018.
[21] U. C. Hasar, "Two novel amplitude-only methods for complex permittivity determination of medium- and low-loss materials," *Meas. Sci. Technol.*, vol. 19, no. 5, Apr. 2008, Art. no. 055706.
[22] U. C. Hasar, "Unique retrieval of complex permittivity of low-loss dielectric materials from transmission-only measurements," *IEEE Geosci. Remote Sens. Lett.*, vol. 8, no. 3, pp. 562–564, May 2011.
[23] T. Ozturk, O. Morikawa, İ. Ünal, and İ. Uluer, "Comparison of free space measurement using a vector network analyzer and low-cost-type THz-TDS measurement methods between 75 and 325 GHz," *J. Infr. Millim. THz Waves*, vol. 38, no. 10, pp. 1241–1251, Oct. 2017.
[24] G. F. Engen and C. A. Hoer, "Thru-reflect-line: An improved technique for calibrationg the dual 6-port automatic network analyzer," *IEEE Trans. Microw. Theory Techn.*, vol. MTT-27, no. 12, pp. 983–987, Dec. 1979.
[25] H.-J. Eul and B. Schiek, "A generalized theory and new calibration procedures for network analyzer self-calibration," *IEEE Trans. Microw. Theory Techn.*, vol. 39, no. 4, pp. 724–731, Apr. 1991.
[26] U. C. Hasar, G. Ozturk, Y. Kaya, and M. Ertugrul, "Calibration-free time-domain free-space permittivity extraction technique," *IEEE Trans. Antennas Propag.*, vol. 70, no. 2, pp. 1565–1568, Feb. 2022.
[27] U. C. Hasar, "Non-destructive testing of hardened cement specimens at microwave frequencies using a simple free-space method," *NDT&E Int.*, vol. 42, no. 6, pp. 550–557, Sep. 2009.
[28] U. C. Hasar, "Elimination of the multiple-solutions ambiguity in permittivity extraction from transmission-only measurements of lossy materials," *Microw. Opt. Technol. Lett.*, vol. 51, no. 2, pp. 337–341, Feb. 2009.
[29] B. Riddle, J. Baker-Jarvis, and J. Krupka, "Complex permittivity measurements of common plastics over variable temperatures," *IEEE Trans. Microw. Theory Techn.*, vol. 51, no. 3, pp. 727–733, Mar. 2003.
[30] D. A. Houtz, D. Gu, and D. K. Walker, "An improved two-port transmission line permittivity and permeability determination method with shorted sample," *IEEE Trans. Microw. Theory Techn.*, vol. 64, no. 11, pp. 3820–3827, Nov. 2016.
[31] U. C. Hasar, "Determination of complex permittivity of low-loss samples from position-invariant transmission and shorted-reflection measurements," *IEEE Trans. Microw. Theory Techn.*, vol. 66, no. 2, pp. 1090–1098, Feb. 2018.
[32] U. C. Hasar, G. Ozturk, J. J. Barroso, T. U. Gurbuz, Y. Kaya, and M. Ertugrul, "Graphical method for examining complex natural frequencies of dispersive materials," *IEEE Microw. Wireless Compon. Lett.*, vol. 31, no. 5, pp. 421–424, May 2021.